DOI: 10.5281/OGP.OAJPM.16876593

Research Article

Open Access Journal of Physics & Mathematics

ISSN: 3068-7527

OPENPUB GLOBAL PUBLISHERS

Received: 21-06-2025 Accepted: 10-07-2025 Published: 26-07-2025

Volume 1 | Issue 2

Dynamics of Cu_2O Rydberg Excitons - Real Density Matrix Approach

Karol Karpiński and Gerard Czajkowski*

Technical University of Bydgoszcz Al., Poland

***Corresponding author:** Gerard Czajkowski, Technical University of Bydgoszcz, Poland.

Citation: Karpiński, K., Czajkowski, G. (2025). Dynamics of Cu_2O Rydberg Excitons - Real Density Matrix Approach. Open Access J. Phys. Math. 1(2): 01-25.

Abstract

Basing on recent reliable measurements of the life- and coherence time of Cu_2O Rydberg excitons, we present an analytical method which enables to describe the experimental results. The real-density matrix approach (RDMA) is applied to describe two-photon absorption in Cu_2O through the excitonic response to the exciting fields. This approach produces an analytical expression for the emission intensity time evolution, and can be used to explain trends in reported experimental data. Our approach takes into account the effect of the coherence between the electron-hole pair and the electromagnetic fields, the quantum beats and the life- and coherence time dependence on the applied laser power. Adding a separation of slow- and rapid dynamics components we find excellent agreement with the experimental data.

Keywords: Rydberg Excitons, Cuprous Oxide, Two Photon Absorption, Exciton Dynamics, Exciton Coherence Times and Lifetimes

1. Introduction

Since the first observation of Rydberg excitons (RE) in Cu_2O [1] they become a subject of intensive studies [2]. The research started from optical properties of REs in natural crystals, then it evaluated towards REs in low dimensional nanostructures [3-5]. Both linear and nonlinear optical properties were examined. The theory, so far, is well-developed and the theoretical results agree well with experimental findings. The majority of experiments and theoretical considerations on the optical properties of Rydberg excitons was devoted to excitons created by a harmonic-time dependent wave of the type $\mathbf{E}(r, t) = \mathbf{E}_0 \exp(i\mathbf{kr}-i\omega t)$ where $\mathbf{E}$ is the electric field vector, ω the frequency (circular frequency) and $\mathbf{k}$ the wave vector. Since the optical functions are represented by time averages, they remain time independent, and the exciton (exciton population) time dependence was not discussed. Recently, the trend changed to experiments and theory on the dynamic processes [6,7], where excitons are created by pulsed excitation. The exciton population, created within a finite time, decays then with a time constant, which is related to the so-called exciton life time.

The relevant equations on excitons created in stationary way contain an number of parameters, and most of them are known (for example electron- and hole effective masses, quantum states oscillator strengths, energy gap, dielectric constant, exciton Rydberg energy etc.) However, there is a one important parameter, which is not exactly known. It is the above mentioned exciton lifetime of a quantum state n (notation T_{2n}, τ_n), which corresponds to an energy $T_n = h/T_{2n}$, also called the damping constant (homogeneous broadening). The coefficients T_n represent dissipative processes that, in general (and we will see it below) are energy and temperature dependent [8-10]. The topic of calculation of exciton lifetime has not been covered yet. There are some estimation, as, for example $T_n \propto (n^2\text{-}1)/n^5$ [12] which gives the tendency $\tau_n \propto n^3$. Very often the damping Γ was assumed as a free parameter, and was determined by fitting experimental results, thus in an indirect way.

In a recent paper the authors reported on a direct measurement of the lifetime and coherence time of Cu_2O Rydberg excitons up to principal quantum number n = 9 [6]. They used a method, where a degenerate two-photon excitation (2PA) generates a one-photon emission at twice the pump energy. They used short (a few ps) laser impulses and the exciton lifetime exceeds the impulse duration. When the impulse vanishes, the excitons decay for each Rydberg state. The slope of the decay rate gives directly the lifetime τ, and

coherence time τ_{coh}, by the relation $\tau_{coh} = 2\tau$. During the decay process one observes oscillations (the so-called quantum beats) due to the interference of the neighboring exciton states. In addition, in the dependence of the lifetime on the laser pump power and the probe temperature, is measured [6]. The general tendency is the decrease of the lifetime with the increase of the pump power (temperature).

Since a two photon excitation is a nonlinear process (a $\chi^{(3)}$ process), in the theoretical description of the above reported process we advance the application of the real density matrix approach (RDMA, also called coherent wave theory). This approach has been successful in describing linear and nonlinear optical properties of semiconductors in terms of Rydberg excitons. Recently it was used in the theoretical description of two photon non-degenerate absorption in silicon, in the case of stationary excitation [11]. Here we extend this approach to the case of degenerate 2PA and finite-time excitation impulses. As compared with earlier works on the application of RDMA to Rydberg physics, the RDMA scheme is supplemented by quantum beatings equations, time-scale separation, and the dependence of exciton lifetime on applied laser power [12].

The paper is organized as follows. In Section 2 we recall the basic equations of the RDMA, adapted to the case of degenerate 2-photon absorption. In Section 3 we explicitly derive the formulas for linear and non- linear susceptibility for a Cu_2O crystal, irradiated by a finite-time pulse. Next, in Section 4 we calculate the exciton life- and coherence times and other parameters needed for intensity calculations. In Section 5 we derive the final expression for the nonlinear time- dependent 2P emission intensity. Finally, in Section 6, we present the Fourier transforms of the theoretical emission intensity. The Appendix contains details of the presented calculation.

2. Two-Photon Absorption in RDMA Formalism

2.1 The Constitutive Equations

In the RDMA approach the bulk nonlinear response will be described by a closed set of differential equations ("constitutive equations"): one for the coherent amplitude $Y(\mathbf{r}_1, \mathbf{r}_2)$ representing the exciton density related to the inter-band transition, one for the density matrix for electrons $\mathbf{C}(\mathbf{r}_1, \mathbf{r}_2)$ (assuming a non- degenerate conduction band), and one for the density matrix for the holes in the valence band, $\mathbf{D}(\mathbf{r}_1, \mathbf{r}_2)$. Below we will use the notation

$$Y(\mathbf{r}_1, \mathbf{r}_2) = Y_{12}, \quad \text{etc}, \tag{1}$$

The constitutive equations have the form: the inter band equation

$$\mathrm{i}\hbar\frac{\partial Y_{12}}{\partial t} - H_{eh}Y_{12} = -\mathbf{M}\mathbf{E}(\mathbf{R}_{12}) + \mathbf{E}_1\mathbf{M}_0C_{12} + \mathbf{E}_2\mathbf{M}_0D_{12} + \mathrm{i}\hbar\left(\frac{\partial Y_{12}}{\partial t}\right)_{\mathrm{irrev}}, \tag{2}$$

conduction band equation

$$\mathrm{i}\hbar\frac{\partial C_{12}}{\partial t} + H_{ee}C_{12} = \mathbf{M}_0(\mathbf{E}_1Y_{12} - \mathbf{E}_2Y_{21}^*) + \mathrm{i}\hbar\left(\frac{\partial C_{12}}{\partial t}\right)_{\mathrm{irrev}}, \tag{3}$$

valence band equation

$$\mathrm{i}\hbar\frac{\partial D_{21}}{\partial t} - H_{hh}D_{21} = \mathbf{M}_0(\mathbf{E}_2Y_{12} - \mathbf{E}_1Y_{21}^*) + \mathrm{i}\hbar\left(\frac{\partial D_{21}}{\partial t}\right)_{\mathrm{irrev}}, \tag{4}$$

where *the operator* H_{eh} is the two-particles (electron and hole) effective mass Hamiltonian

$$H_{eh} = E_g - \frac{\hbar^2}{2M_{tot}}\partial_Z^2 - \frac{\hbar^2}{2M_{tot}}\nabla_{R_\parallel}^2 - \frac{\hbar^2}{2\mu}\partial_z^2 - \frac{\hbar^2}{2\mu}\nabla_\rho^2 + V_{eh}, \quad (5)$$

with the separation of the center-of-mass coordinate R from the relative coordinate ρ on the plane $x - y$,

$$H_{ee} = -\frac{\hbar^2}{2m_e}(\nabla_1^2 - \nabla_2^2),$$
$$H_{hh} = -\frac{\hbar^2}{2m_h}(\nabla_1^2 - \nabla_2^2), \quad (6)$$

and E_{12} means that the wave electric field in the medium is taken in a middle point between $\mathbf{r}_1$ and $\mathbf{r}_2$: we take them at the center-of-mass

$$\mathbf{R} = \mathbf{R}_{12} = \frac{m_h\mathbf{r}_1 + m_e\mathbf{r}_2}{m_h + m_e}. \quad (7)$$

In the above formulas m_e, m_h are the electron and the hole effective masses (more generally, the effective mass tensors), M_{tot} is the total exciton mass, and μ the reduced mass of electron-hole pair. The smeared- out transition dipole density **M**(**r**) is related to the bi- locality of the amplitude Y and describes the quantum coherence between the macroscopic electromagnetic field and the inter-band transitions [4]. The terms $(\partial Y/\partial t)_{irrev}$ etc. describe the irreversible dissipation and radiation decay processes due to all dephasing processes. The resulting coherent amplitude Y12 determines the excitonic part of the polarization of the medium

$$\mathbf{P}(\mathbf{R},t) = 2\int \mathrm{d}^3 r\, \mathbf{M}^*(\mathbf{r})\mathrm{Re}\; Y(\mathbf{R},\mathbf{r},t)$$
$$= \int \mathrm{d}^3 r \mathbf{M}^*(\mathbf{r})[Y(\mathbf{R},\mathbf{r},t) + \mathrm{c.c}], \quad (8)$$

where $\mathbf{r} = \mathbf{r}_1 - \mathbf{r}_2$ is the electron-hole relative coordinate. Having in mind experiments described in [6], we consider a situation where the irradiating electromagnetic field **E** includes two frequencies ω_1 and ω_2, and is written as

$$\mathbf{E} = \mathbf{e}_\alpha F(t)\Big[\boldsymbol{\mathcal{E}}_{01}\exp(\mathrm{i}\mathbf{k}_1\mathbf{R} - \mathrm{i}\omega_1 t)$$
$$+ \boldsymbol{\mathcal{E}}_{02}\exp(\mathrm{i}\mathbf{k}_2\mathbf{R} - \mathrm{i}\omega_2 t) + \mathrm{c.c.}\Big], \quad (9)$$

with the envelope function *F (t)* (the impulse shape, the definition will be given below), and

$$|\mathbf{k}_j| = \frac{\omega_j}{c}\sqrt{\epsilon(\omega_j)} = n_j\frac{\omega_j}{c}, \quad j = 1,2, \quad (10)$$

and n_j are refractive indices at the frequencies ω_j.

In the following, we consider only one component $(\mathbf{A})_\alpha$ of the vectors **E, P** and **M.** The linear optical properties are calculated by solving the inter band equation (2), supplemented by the corresponding Maxwell equation, where the polarization (8) acts as a source. For computing the nonlinear optical properties we use the entire set of constitutive equations (2-4). Although finding a general solution of the equations is challenging, in special situations a solution can be found. For example, if one assumes that the matrices *Y, C* and *D* can be expanded in powers of the electric field **E**, an iterative procedure can be used. In general, solving for *Y,C* and *D* in the context of two- photon absorption depends on the relation between the incoming frequencies ω_1, ω_2 (and thus energies $\hbar\omega_1$, $\hbar\omega_2$) and the fundamental gap energy E_g, which enters as a parameter in the electron-hole Hamiltonian.

We consider the case, when
$\hbar\omega_1 + \hbar\omega_2 \leq E_g$, the excitation of discrete excitonic states is possible.

2.2 The Iterative Solution of Constitutive Equations

Our goal is to derive expressions for the two-photon absorption coefficients. These can be obtained from the third-order nonlinear susceptibility, which, in turn, can be determined via an iterative procedure within the context of the RDMA. To apply the iteration procedure we assume, that the relevant quantities *P, Y, C* and *D* can be expanded in series of the input electric field amplitudes. The considered inter-band transition is composed of two steps. The first step starts from the initial state E_i (here the maximum E_y of the valence band) to an intermediate (virtual) state β, the second is from the state β to the final state E_f (the minimum of the conduction band E_c. The first step in the iteration consists of solving the equation (2), which at this stage takes on the form

$$\mathrm{i}\frac{\partial Y^{(1)}}{\partial t} - H_{eh}^{(j)} Y^{(1)} = -\mathbf{ME} + \mathrm{i}\hbar \left(\frac{\partial Y^{(1)}}{\partial t}\right)_{\mathrm{irrev}}, \quad (11)$$

where E has the form (9). The Hamiltonians $H_{j,eh}$ are defined with regard to the two steps of transition described above:

$$H_{1,eh} = E_\beta - E_v + H_r, \quad (12)$$

$$H_{2,eh} = E_c - E_\beta + H_r, \quad (13)$$

$$H_r = \left(-\frac{\hbar^2}{2}\right) \boldsymbol{\nabla}_r \left(\underline{\underline{\mu}}\right)^{-1} \boldsymbol{\nabla}_r + V(\mathbf{r}), \quad (14)$$

"where μ is the exciton reduced mass tensor for given pair of bands

=

C and *V*, and *V(***r***)* the dielectrically screened electron-hole Coulomb potential, E_β is the energy of the virtual band, and $E_c E_v$ correspond to extreme od valence and conduction bands". When considering the time evolution of the exciton population, generate by the impulse (9), two time scales should be accounted for. The processes of exciton creation are rapid processes, on the femtosecond scale. The time characterizing the decline process of the population is proportional to the lifetime τ , which is of the order $\tau < 20$ ps, i.e. is a slow process. Therefore the amplitudes $Y^{(1)}_j$ will consist of two parts

$$Y_j^{(1)}(\mathbf{r}, t) = Y_{\mathrm{slow}}^{(1)}(t) Y_{0j}(\mathbf{r}) \mathrm{e}^{-\mathrm{i}\omega_j t}. \quad (15)$$

For the irreversible part we assume the simple form

$$\left(\frac{\partial Y^{(1)}}{\partial t}\right)_{\mathrm{irrev}} = -\frac{1}{\tau} Y^{(1)}. \quad (16)$$

As follows from experiments, the decline of excitonic absorption is governed by the rule $\propto \exp(-t/\tau_{n\ell m})$. To obtain this behavior, we distinguish slow and fast changes (in other words, two time scales) in the excitonic amplitudes *Y* and matrices *C,D*. With regard to (9), we put into (11), obtaining

$$Y^{(1)} = \tilde{Y} e^{-\mathrm{i}\omega t} \quad (17)$$

$$\frac{\mathrm{d}\tilde{Y}}{\mathrm{d}t} = -\mathrm{i}\omega \tilde{Y} \mathrm{e}^{-\mathrm{i}\omega t} + e^{-\mathrm{i}\omega t} \frac{\mathrm{d}\tilde{Y}}{\mathrm{d}t} + e^{-\mathrm{i}\omega t} \mathrm{i}\Omega_{eh} \tilde{Y}$$

$$- e^{-\mathrm{i}\omega t} \left(\frac{\mathrm{d}\tilde{Y}}{\mathrm{d}t}\right)_{\mathrm{irrev}} = \frac{\mathrm{i}}{2\hbar} F(t) e^{-\mathrm{i}\omega t} M(\mathbf{r}), \quad (18)$$

$$\mathrm{i}(\Omega_{eh} - \omega)\tilde{Y} + \frac{\mathrm{d}\tilde{Y}}{\mathrm{d}t} - \left(\frac{\mathrm{d}\tilde{Y}}{\mathrm{d}t}\right)_{\mathrm{irrev}} = \frac{\mathrm{i}}{2\hbar} F(t) M(\mathbf{r}).$$

Taking the 2 steps in 2-photon process, we have two pairs of equations

$$i\hbar\left[i\omega_1+\frac{1}{\tau}\right]Y_{1+}^{(1)}-H_{eh}^{(1)}Y_{1+}^{(1)}=-M\mathcal{E}_{01}^{*},\qquad(19)$$
$$i\hbar\left[-i\omega_1+\frac{1}{\tau}\right]Y_{1-}^{(1)}-H_{eh}^{(1)}Y_{1-}^{(1)}=-M\mathcal{E}_{01},$$

with similar equations for $Y_{2\pm}^{(1)}$, M is the relevant component of the transition dipole density. Now we separate the slow and rapid processes, by putting

$$\tilde{Y}^{(1)}=Y_{0j\pm}^{(1)}(\mathbf{r})Y_{\text{slow}}^{(1)}\qquad(20)$$

In what follows we consider only the resonant part. The parts $Y_{0j-}^{(1)}$ correspond to rapid processes, and have the form

$$Y_{01-}^{(1)}(\mathbf{r})=\mathcal{E}_{01}\sum_{n\ell m}\frac{c_{n\ell m}\varphi_{n\ell m}(\mathbf{r})}{E_\beta+E_{n\ell m}-\hbar\omega_1-i\hbar\tau_{n\ell m}^{-1}},$$
$$Y_{02-}^{(1)}(\mathbf{r})=\mathcal{E}_{02}\sum_{n\ell m}\frac{c_{n\ell m}\varphi_{n\ell m}(\mathbf{r})}{E_c-E_\beta+E_{n\ell m}-\hbar\omega_2-i\hbar\tau_{n\ell m}^{-1}},$$
$$E_\beta=E_v+\hbar\omega_1,\qquad(21)$$

where $E_v E_c$ are the extreme of the valence and conduction bands, respectively. The coefficients $c_{n`m}$ and eigenfunctions are defined as follows

$$c_{n\ell m}=\int d^3rM(\mathbf{r})\varphi_{n\ell m}(\mathbf{r}),$$
$$\varphi_{n\ell m}=R_{n\ell}(r)Y_{\ell m}(\theta,\phi),\qquad(22)$$

Y_{lm} are the spherical harmonics, R_{nl} are the radial functions of a corresponding hydrogen atom-like Schrödinger equation,

$$\varphi_{n\ell m}(\mathbf{r})=R_{n\ell m}(r)Y_{\ell m}(\theta,\phi),\qquad(23)$$

where

$$R_{n\ell m}(r)=N_{n\ell}\left(\frac{2\eta_{\ell m}r}{na^*}\right)^\ell$$
$$\times M\left(-n+\ell+1;2\ell+2;\frac{2\eta_{\ell m}r}{na^*}\right)e^{-\eta_{\ell m}r/na^*},\qquad(24)$$
$$N_{n\ell}=\frac{1}{(2\ell+1)!}\left[\frac{(n+\ell)!}{2n(n-\ell-1)!}\right]^{1/2}\left(\frac{2}{n}\right)^{3/2}.$$

In the above expression M(*a;b;z*) is the confluent hypergeometric function. The energy eigenvalues related to the eigenfunctions (23) have the form

$$E_{n\ell m}=-\frac{\eta_{\ell m}^2}{n^2}R^*,\qquad(25)$$

Where

$$n=1,2,\ldots,\quad \ell=0,1,2,\ldots n-1,$$
$$m=-\ell,-\ell+1,\ldots,+\ell,\qquad(26)$$

R^* is the effective exciton Rydberg energy for the exciton

$$R^*=\frac{\mu_\parallel e^4}{2(4\pi\epsilon_0\epsilon_b)^2\hbar^2},\qquad(27)$$

the anisotropy parameter γ is defined as

$$\gamma = \frac{\mu_{\|}}{\mu_z,} \qquad (28)$$

$\mu_{\|}$ and $\mu_z$are the heavy hole exciton reduced masses in the x-y plane and in the z-direction, respectively,

$$\frac{1}{\mu_{\|}} = \frac{1}{m_{e\|}} + \frac{1}{m_{h\|}},$$
$$\frac{1}{\mu_z} = \frac{1}{m_{ez}} + \frac{1}{m_{hz}}. \qquad (29)$$

$_0$ is the vacuum dielectric constant, and $\varepsilon_{\ell m}$ are relative dielectric tensor elements. The quantity $\eta_{\ell m}(\gamma)$is given by the following expression [13]

$$\eta_{\ell m}(\gamma) = \int_0^{2\pi} \mathrm{d}\phi \int_0^{\pi} \frac{|Y_{\ell m}|^2 \sin\theta \mathrm{d}\theta}{\sqrt{\sin^2\theta + \gamma\cos^2\theta}}. \qquad (30)$$

With regard to (25), the excitonic resonance energies result from equation

$$E_{Tn\ell m} = E_g + E_{n\ell m}. \qquad (31)$$

The slow part $Y^{(1)}_{slow}$slow satisfies the equation

$$\frac{\mathrm{d}Y^{(1)}_{\mathrm{slow}}}{\mathrm{d}t} - \left(\frac{\mathrm{d}Y^{(1)}_{\mathrm{slow}}}{\mathrm{d}t}\right)_{\mathrm{irrev}} = F(t), \qquad (32)$$

as previously, *F(t)* describes the exciting impulse profile, and

$$\left(\frac{\mathrm{d}Y^{(1)}_{slow}}{\mathrm{d}t}\right)_{\mathrm{irrev}} = -\sigma Y^{(1)}_{\mathrm{slow}}, \qquad (33)$$

where, to simplify the notation, we put $\sigma = 1/\tau_{n\ell m}$. Equation (32) can be solved by means of Green's function, satisfying the equation

$$\frac{\mathrm{d}G(t,t')}{\mathrm{d}t} + \sigma G(t,t') = -\delta(t-t'), \qquad (34)$$

with the solution

$$G(t,t') = \frac{1}{2\sigma}\mathrm{e}^{-\sigma|t-t'|}. \qquad (35)$$

Thus, the solution of (32) has the form

$$Y^{(1)}_{\mathrm{slow}}(t) = \int_{-\infty}^{\infty} F(t')G(t,t')\,\mathrm{d}t'. \qquad (36)$$

As follows from the definition of σ, $Y^{(1)}_{\mathrm{slow}}$ slow will be labelled by quantum numbers *n;l;m.*

2.3 Coherence Time and Exciton Life Time

The values of the above mentioned exciton life time can be taken from experiments [6] Table I.) We can also estimate them, using the relation between the coherence time and the exciton life time. Coherence time is the time duration over which the medium

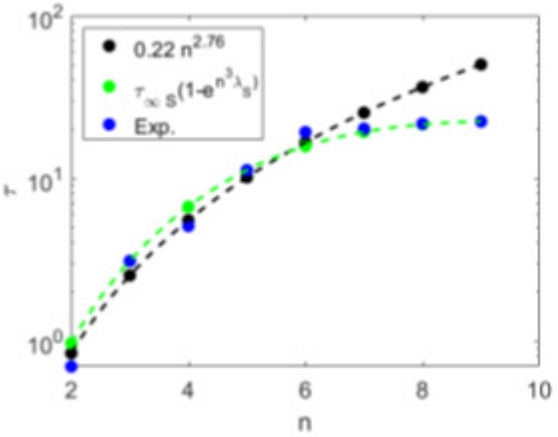

Figure 1: Exciton lifetimes, directly measured S states lifetimes [6] (blue dots), in good agreement with the n2.7 scaling (black dashes), up to n = 6,(42), for n > 6 good agreement with scaling (43) for S excitons

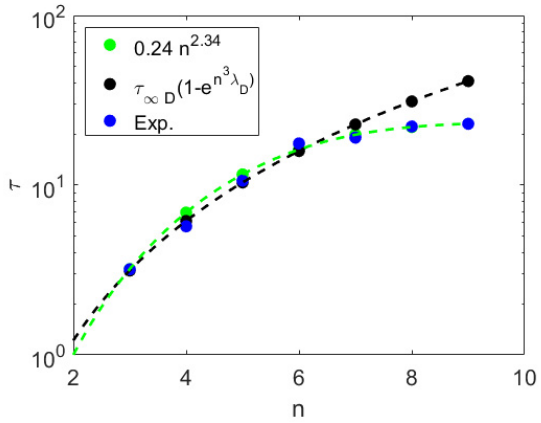

Figure 2: The same as Figure 1, for D2 states, for n ≤ 6 in good agreement with n3 scaling, for n > 6 good agreement with (43) for D excitons

impulse response is considered to be not varying. The coherence time, which we denote as τ_{coh}, is calculated by dividing the coherence length by the phase velocity of light in a medium; approximately given by

$$\tau_{\mathrm{coh}} = \frac{1}{\Delta\nu} \approx \frac{\lambda^2}{c\,\Delta\lambda}, \qquad (37)$$

where λ is the central wavelength of the source, Δν and Δλ is the spectral width of the source in units of frequency and wavelength respectively, and c is the speed of light in vacuum. Identifying the variation of impulse response with energy difference between neighboring exciton states we obtain (without specification to S or D states)

$$\tau_{\mathrm{coh},n} = \frac{\delta\hbar}{E_{n+1} - E_n}, \qquad (38)$$

where δ is a certain parameter. Below we take the values δ_S = 19.7 and δ_{D1} = 19.73, δ_{D2} = 18.72, for S and D1,D2 excitons, respectively, which give a fairly good agreement of theoretical and experimental values of exciton life times. If the energies are given in meV, we obtain the result in picoseconds

$$\tau_{\mathrm{coh},n} = \frac{2\delta\hbar}{E_{n+1} - E_n}. \qquad (39)$$

On the other hand, we have the relation

$$\tau_{coh,n} = 2\tau_n, \qquad (40)$$

τ_n being exciton lifetimes. By equations (39, 40) we obtain the lifetimes

$$\tau_{n00} = \frac{\delta_S \hbar}{E_{n+1,00} - E_{n00}} = \frac{\delta_S \hbar n^2(n+1)^2}{R^* \eta_{00}^2 (2n+1)},$$
$$\tau_{n22} = \frac{\delta_D \hbar}{E_{n+1,22} - E_{n22}} = \frac{\delta_D \hbar n^2(n+1)^2}{R^* \eta_{22}^2 (2n+1)}. \qquad (41)$$

The results for the S states $2 \leq n \leq 9$, and D states $3 \leq n \leq 9$ are given in Tables A1 and A2. We observe a fairly good agreement with the experimental data for the states $n \leq 7$. In this interval the lifetimes scale approximately as

$\tau_{n00} = \tau_{0S} \times n^{2.7}$, S excitons
$\tau_{n22,1} = \tau_{0D1} \times n^{2.7}$, D1 excitons, (42)
$\tau_{n22,2} = \tau_{0D2} \times n^3$, D2 excitons,

where $\tau_{0S} = 0.13, \tau_{0D1} = 0.15, \tau_{0D2} = 0.11$. The formula for D2 exciton is identical as the formula for the case of P excitons in Cu_2O used in [14]. The expressions (42) correspond to the scaling with quantum defects [6]. As observed in experiments, the values of lifetimes for $n > 7$ arrive at a plateau. For higher states states we observe a slow increase, tending to a value $\tau\infty$. The scaling in this interval can be described by the formula

$$\tau_{n00} = \tau_{nS} = \tau_{\infty S}\left(1 - e^{-n^3 \lambda_S}\right), \quad \text{S excitons,}$$
$$\tau_{nD1,2} = \tau_{\infty D1,2}\left((1 - e^{-n^3 \lambda_{D1,2}}\right), \quad \text{D1,D2 excitons.} \qquad (43)$$

The results, for

$\tau\infty S = 22.89$ ps, $\lambda S = 5.36 \times 10{-}3$, (44)
$\tau\infty D1 = 23.65$ ps, $\lambda D1 = 5.386 \times 10{-}3$,
$\tau\infty D2 = 23.14$ ps, 25; $\lambda_{D2} = 6.6 \times 10^{-3}$, (45)

are given in Tables A1 and A1. The above data include the splitting into D1 and D2 excitons. The switching between the increasing of *T* (those decreasing of intensity) can be explained as follows [15]. As we have shown above, the absorption spectrum for energies below the energy gap consists of a series of lines at energy values (31) with intensities decreasing, roughly speaking, as $1/n^3$ (those exciton lifetimes increasing, see (42)). For high values of the quantum number *n* (i.e. for energies just below the gap), the density of exciton states per unit energy is

$$D(E) = 2\frac{\partial n}{\partial E} = \frac{2n^3}{R^*} \qquad (46)$$

and, since the density decreases as $1/n^3$, we obtain a finite limit in the absorption coefficient, represented above by the quantity τ_∞, for energies near E_g.

2.4 Quantum beats

In experimental intensity curves shown in Ref. [6] some oscillations, also called quantum beats, around the smooth shape determined by a function *F(t)* are observed. There are several types of oscillations, with different frequencies with different periodicity and amplitudes. As we show below, the oscillations are due to interference between quantum mechanical waves, generated by neighboring states, in the region of an exciton state n (S or D). Consider, for example, states |300>, |322 >, and |400 >, denoted further by 1,2, and 3. The state of the system is described by three waves

$$\Psi(\mathbf{r},t) = a_1\psi_1(\mathbf{r})\exp(-i\Omega_1 t) + a_2\psi_2(r)\exp(i\Omega_2 t) + a_3\psi_1(\mathbf{r})\exp(i\Omega_3 t), \qquad (47)$$

where a_1, a_2, a_3 are real numbers such that

$$a_1^2 + a_2^2 + a_3^2 = 1, \qquad (48)$$

$\psi_i(r)$, $i = 1, 2, 3$ are real valued functions, and

$$\Omega_1 = \frac{E_1}{\hbar}, \quad \Omega_2 = \frac{E_2}{\hbar}, \quad \Omega_3 = \frac{E_3}{\hbar}. \qquad (49)$$

The density of probability, that the system is in a non- stationary state described by (47), is given by

$$\begin{aligned}\rho(\mathbf{r},t) &= a_1^2\psi_1^2(\mathbf{r}) + a_2^2\psi_2^2(\mathbf{r}) + a_3^2\psi_3^2(\mathbf{r}) \\ &+ 2a_1a_2\psi_1(\mathbf{r})\psi_2(\mathbf{r})\cos(\Omega_{12}t) \\ &+ 2a_1a_3\psi_1(\mathbf{r})\psi_3(\mathbf{r})\cos(\Omega_{13}t) \\ &+ 2a_2a_3\psi_2(\mathbf{r})\psi_3(\mathbf{r})\cos(\Omega_{23}t),\end{aligned} \qquad (50)$$

where

$$\Omega_{ij} = \frac{E_i - E_j}{\hbar}. \qquad (51)$$

The quantum beats are attributed to transitions between neighboring S and D states $|n00\rangle$, $|n22\rangle$, $|(n+1, 00\rangle$. Their periodicity is given by the equations

$$\begin{aligned}\tau_{qbS,i} &= \left|\frac{2\pi\hbar}{E_{n00} - E_{n+1,00}}\right|, \\ \tau_{qbD,i} &= \left|\frac{2\pi\hbar}{E_{n22} - E_{n+1,22}}\right|, \\ \tau_{qbSD,i} &= \left|\frac{2\pi\hbar}{E_{i00} - E_{n22}}\right|, \quad i = n,\ n+1.\end{aligned} \qquad (52)$$

The impact of quantum beats on the exciton spectra will be described by expressions of the type (50). The over-all expression for the oscillating

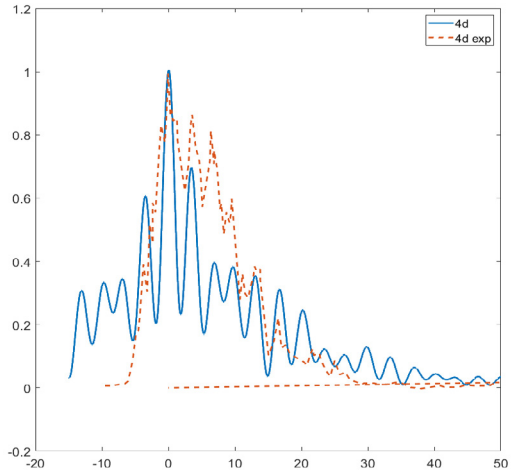

Figure 3: Linear time dependent emission, showing quantum beats for 4D2 excitons, the experimental curve from [6]

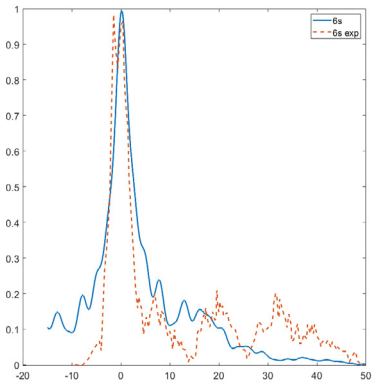

Figure 4: Linear time dependent emission, showing quantum beats) for 6S excitons

will be described by expressions of the type (50). The over-all expression for the oscillating terms will be taken in the form [6]

$$\psi_{osc,n}(t) = \frac{Q_n}{2}\left[1 + \sum_j q_{jn}\cos(\Omega_{jn}t)\right], \qquad (53)$$

where *j* runs over the inter-exciton states transitions starting with nS(nD) accounted for. The quantum beats amplitudes q_{jn} are proportional to the quadrupole transitions moments Q_{jn}, given in [8],

$$q_{jn} = \frac{Q_{jn}}{Q_n}, \quad Q_n = \sum_j Q_{jn}. \qquad (54)$$

3. Linear and Nonlinear Susceptibility

3.1 Linear Susceptibility

The above consideration allow to calculate the total excitonic optical response in the 2 photon absorption process. This will be obtained by means of linear and nonlinear excitonic amplitudes $Y_{j-}^{(1)}(t)$ and $Y_{j-}^{(3)}(t)$.

The linear amplitudes have the form

$$Y_{1-}^{(1)}(\mathbf{r},t) = \mathcal{E}_{01}\sum_{n\ell m}\frac{c_{n\ell m}\varphi_{n\ell m}(\mathbf{r})}{E_\beta - \hbar\omega_1 + E_{n\ell m} + \mathrm{i}\hbar/\tau_{n\ell m}} \times \psi_{osc,n\ell m}(t), \qquad (55)$$

with analogous formula for " $Y_{2-}^{(1)}(t)$. We use" the notation

$$\left(G(t,t')F(t')\right) = \int_{-\infty}^{\infty} G(t,t')F(t')\mathrm{d}t'. \qquad (56)$$

The solutions for $Y_{j\pm}^{(1)}(t)$determined above allow the calculation of the linear polarization being a function of time *t*

$$P^{(1)}(\omega_1,\omega_2;t) = \int \mathrm{d}^3 r \left[Y_{1-}^{(1)} + Y_{1+}^{(1)*}\right] M^*(\mathbf{r})$$
$$+ \int \mathrm{d}^3 r \left[Y_{2-}^{(1)} + Y_{2+}^{(1)*}\right] M^*(\mathbf{r}) \qquad (57)$$
$$= \epsilon_0 \chi^{(1)}(\omega_1;t)\mathcal{E}_{01} + \epsilon_0 \chi^{(1)}(\omega_2;t)\mathcal{E}_{02},$$

where

$$\chi^{(1)}(\omega_1;t) = \frac{2}{\epsilon_0}\sum_{n\ell m}\Big\{\psi_{osc,n}(t)\big(G_{n\ell m}(t,t')F(t')\big)$$
$$\times \frac{|c_{n\ell m}|^2(E_{n\ell m}+E_\beta)}{(E_\beta+E_{n\ell m})^2 - \hbar^2(\omega_1+\mathrm{i}/\tau_{n\ell m})^2}\Big\}, \qquad (58)$$
$$\chi^{(1)}(\omega_2;t) = \frac{2}{\epsilon_0}\sum_{n\ell m}\Big\{\psi_{osc,n}(t)\big(G_{n\ell m}(t,t')F(t')\big)$$
$$\times \frac{|c_{n\ell m}|^2(E_{n\ell m}+E_g)}{(E_g+E_{n\ell m})^2 - \hbar^2[(\omega_1+\omega_2)+\mathrm{i}/\tau_{n\ell m}]^2}\Big\}.$$

3.2 Nonlinear Susceptibility

In order to obtain the nonlinear response, the solutions for $Y_{j,\pm}^{(1)}(t)$ (not $Y_{j,pm}^{(1)}(t)$). are inserted as a source term in the conduction band equation (3) and the valence band equation (4). Note that each of these equations depend on the electromagnetic field. If the irreversible terms are well defined, the equations (3,4) can be solved, and this second step of the iteration yields expressions for the density matrices C and D. We use for the irreversible terms a linear relaxation time approximation

$$\left(\frac{\partial C}{\partial t}\right)_{\text{irrev}} \qquad (59)$$
$$= -\frac{1}{T_1}\left[C(\mathbf{X},\mathbf{r},t) - f_{0e}(\mathbf{r})C(\mathbf{X},\mathbf{r}=0,t)\right] - \frac{C(0)}{T_1},$$

"where $\mathbf{X} = (\mathbf{r}_1+\mathbf{r}_2)/2$, T_1 is the carrier relaxation time, and f_{0e}, f_{0h} are normalized Boltzmann distributions". for electrons and holes, respectively,

$$f_{0e}(\mathbf{r}) = \int \mathrm{d}^3 q f_{0e}(\mathbf{q}) e^{-\mathrm{iqr}} \qquad (60)$$
$$= \exp\left(-\frac{m_{e\|}k_B\mathcal{T}}{2\hbar^2}\rho^2 - \frac{m_{ez}k_B\mathcal{T}}{2\hbar^2}z^2\right),$$

where k_B is the Boltzmann constant, and T the temperature. The same type of expression holds for the holes. From (59) one obtains the solutions in the form

$$C(\mathbf{r},t) = -\frac{i}{\hbar}T_1 f_{0e}(\mathbf{r})J_C(0),$$
$$D(\mathbf{r},t) = -\frac{\mathrm{i}}{\hbar}T_1 f_{0h}(\mathbf{r})J_D(0), \qquad (61)$$

where we present an approximation following from the assumption $T_1 \gg T_2$. The sources terms J_C; J_D are defined as

$$J_C = M_0\mathcal{E}(Y_{12} - Y_{12}^*)$$
$$= 2iM_0F(t)|\mathcal{E}_{01}|^2[\mathrm{Im}\, g(-\omega_1,\mathbf{r}) + \mathrm{Im}\, g(\omega_1,\mathbf{r})]$$
$$+ 2iM_0F(t)|\mathcal{E}_{02}|^2[\mathrm{Im}\, g(-\omega_2,\mathbf{r}) + \mathrm{Im} g(\omega_2,\mathbf{r})], \quad (62)$$

where

$$g(-\omega_1,\mathbf{r}) = \sum_{n\ell m} \frac{c_{n\ell m}\varphi_{n\ell m}(\mathbf{r})}{E_\beta + E_{n\ell m} - \hbar\omega_1 - i\hbar/\tau_{n\ell m}} \times \big(G(t,t')F(t')\big)\psi_{osc,n\ell m} \tag{63}$$

$$g(-\omega_2,\mathbf{r}) = \sum_{n\ell m} \frac{c_{n\ell m}\varphi_{n\ell m}(\mathbf{r})}{E_g + E_{n\ell m} - \hbar(\omega_1+\omega_2) - i\hbar/\tau_{n\ell m}} \times \frac{\tau_{n\ell m}}{2}\big(G(t,t')F(t')\big)\psi_{osc,n\ell m},$$

and $J_c = J_D$. The above expressions can then, in turn, be used as source term for equation (2), which can which can be solved to obtain expressions for $Y^{(3)}_{1,2\pm}$ in the final step of the iteration. Now the equations for the third order coherent amplitudes $Y^{(3)}_{j\pm}$ have the form

$$\begin{aligned} &i\hbar\left(i\omega_1 + \frac{1}{\tau}\right)Y^{(3)}_{1+} - H_{1,eh}Y^{(3)}_{1+} \\ &= M_0(E^*C + E^*D) = E^*(\mathbf{R},t)\tilde{J}, \end{aligned} \tag{64}$$

$$\begin{aligned} &i\hbar\left(-i\omega_1 + \frac{1}{\tau}\right)Y^{(3)}_{1-} - H_{eh}Y^{(3)}_{1-} \\ &= M_0(EC + ED) = E\mathbf{R},t)\tilde{J}, \end{aligned}$$

with similar equations for $Y^{(3)}_{2\pm}$ where

$$\tilde{J} = -\frac{i}{\hbar}M_0\left[T_1 J_C(0) f_{0e}(\mathbf{r}) + T_1 J_V(0) f_{0h}(\mathbf{r})\right]. \tag{65}$$

Equations (64) will be solved by using the same method as in the case of linear amplitudes $Y^{(1)}$. We put $Y^{(3)}$ into the form

$$Y^{(3)} = Y^{(3)}_{slow}Y^{(3)}_0(\mathbf{r}). \tag{66}$$

In analogy to definition (21), the stationary part of $Y^{(3)}$ will be assumed in the form

$$\begin{aligned} Y^{(3)}_{01-}(\mathbf{r}) &= \mathcal{E}_{01}\sum_{\nu\lambda\mu}\frac{d_{\nu\lambda\mu,1}\varphi_{\nu\lambda\mu}(\mathbf{r})}{E_\beta + E_{\nu\lambda\mu} - \hbar\omega_1 - i\hbar/\tau_{\nu\lambda\mu}}, \\ Y^{(3)}_{02-}(\mathbf{r}) &= \mathcal{E}_{02}\sum_{\nu\lambda\mu}\frac{d_{\nu\lambda\mu,2}\varphi_{\nu\lambda\mu}(\mathbf{r})}{E_c - E_\beta + E_{\nu\lambda\mu} - \hbar\omega_2 - i\hbar/\tau_{\nu\lambda\mu}}, \\ E_\beta &= E_v + \hbar\omega_1. \end{aligned} \tag{67}$$

If neglecting the anti-resonant terms, we obtain

$$
\begin{aligned}
d_{\lambda\mu\nu,1} &= \frac{\mathrm{i}M_0T_1}{\hbar}[\langle\varphi_{\lambda\mu\nu}|f_{0e}\rangle + \langle\varphi_{\lambda\mu\nu}|f_{0h}\rangle]2(E_{\nu\lambda\mu}+E_\beta)J_c(0)\\
&= \frac{\mathrm{i}M_0T_1}{\hbar}[\langle\varphi_{\lambda\mu\nu}|f_{0e}\rangle + \langle\varphi_{\lambda\mu\nu}|f_{0h}\rangle]2(E_{\nu\lambda\mu}+E_\beta)\\
&\times 2\mathrm{i}M_0|\mathcal{E}_{01}|^2\sum_{n\ell m}\frac{\hbar}{\tau_{n\ell m}}\frac{c_{n\ell m}\varphi_{n\ell m}(0)}{(E_\beta+E_{n\ell m})^2-\hbar^2(\omega_1+i/\tau_{n\ell m})^2},\\
&= -M_0^2(A_{\lambda\mu\nu}+B_{\lambda\mu\nu})(E_{\nu\lambda\mu}+E_\beta)\\
&\times|\mathcal{E}_{01}|^2\sum_{n\ell m}\frac{T_1}{\tau_{n\ell m}}\frac{c_{n\ell m}\varphi_{n\ell m}(0)}{(E_\beta+E_{n\ell m})^2-\hbar^2(\omega_1+\mathrm{i}/\tau_{n\ell m})^2},
\end{aligned}
\tag{68}
$$

$$
\begin{aligned}
d_{\mu\nu\lambda,2} &= -4M_0^2(A_{\lambda\mu\nu}+B_{\lambda\mu\nu})(E_{\nu\lambda\mu}+E_g)\\
&\times|\mathcal{E}_{02}|^2\sum_{n\ell m}\frac{T_1}{\tau_{n\ell m}}\frac{c_{n\ell m}\varphi_{n\ell m}(0)}{(E_g+E_{n\ell m})^2-\hbar^2(\omega_1+\omega_2+\mathrm{i}/\tau_{n\ell m})^2},
\end{aligned}
$$

where

$$
\begin{aligned}
A_{\lambda\mu\nu} &= \langle\varphi_{\lambda\mu\nu}|f_{0e}\rangle,\\
B_{\lambda\mu\nu} &= \langle\varphi_{\lambda\mu\nu}|f_{0h}\rangle.
\end{aligned}
\tag{69}
$$

The slow part $Y^{(3)}_{slow}$ satisfies the equation

$$
\begin{aligned}
&\frac{\mathrm{d}Y^{(3)}_{\mathrm{slow}}}{\mathrm{d}t} - \left(\frac{\mathrm{d}Y^{(3)}_{\mathrm{slow}}}{\mathrm{d}t}\right)_{\mathrm{irrev}} = F(t)\big(G(t,t')F(t')\big),\\
&Y^{(3)}_{\mathrm{slow}} = \big(G(t,t'')F(t'')\big)\big(G(t'',t')F(t')\big).
\end{aligned}
$$

From $Y^{(3)}_{1\pm}(t), Y^{(3)}_{2\pm}(t)$ one finds the third order polarization according to

$$
\begin{aligned}
P^{(3)}(\omega_1,\omega_2;t) &= \int \mathrm{d}^3r\left[Y^{(3)}_{1-}+Y^{(3)*}_{1+}\right]M^*(\mathbf{r})\\
&+\int \mathrm{d}^3r\left[Y^{(3)}_{2-}(t)+Y^{(3)*}_{2+}(t)\right]M^*(\mathbf{r})\\
&= \epsilon_0\chi^{(3)}(\omega_1,t)|\mathcal{E}_{01}|^2\mathcal{E}_{01}+\epsilon_0\chi^{(3)}(\omega_2,t)|\mathcal{E}_{02}|^2\mathcal{E}_{02}.
\end{aligned}
\tag{70}
$$

where the nonlinear susceptibilities have the form

$$
\begin{aligned}
&\chi^{(3)}(\omega_1,t)\\
&= -\frac{2M_0^2}{\epsilon_0}\sum_{\lambda\mu\nu}\frac{c_{\lambda\mu\nu}(A_{\lambda\mu\nu}+B_{\lambda\mu\nu})(E_{\lambda\mu\nu}+E_\beta)}{(E_\beta+E_{\lambda\mu\nu}-\hbar\omega_1)^2+(\hbar/\tau_{\lambda\mu\nu})^2}\\
&\times\sum_{n\ell m}\frac{T_1}{\tau_{n\ell m}}\frac{c_{n\ell m}\varphi_{n\ell m}(0)}{(E_\beta+E_{n\ell m})^2-\hbar^2(\omega_1+\mathrm{i}/\tau_{n\ell m})^2}\\
&\times\big(G_{\lambda\mu\nu}(t,t'')F(t'')\big)\big(G_{n\ell m}(t'',t')F(t')\big)\psi^2_{osc,\lambda\mu\nu}(t),
\end{aligned}
\tag{71}
$$

$$
\begin{aligned}
&\chi^{(3)}(\omega_2,t)\\
&= -\frac{2M_0^2}{\epsilon_0}\sum_{\lambda\mu\nu}\frac{c_{\lambda\mu\nu}(A_{\lambda\mu\nu}+B_{\lambda\mu\nu})(E_{\nu\lambda\mu}+E_g)}{[E_g+E_{\lambda\mu\nu}-(\hbar\omega_1+\hbar\omega_2)]^2+(\hbar/\tau_{\lambda\mu\nu})^2}\\
&\times\sum_{n\ell m}\frac{T_1}{\tau_{n\ell m}}\frac{c_{n\ell m}\varphi_{n\ell m}(0)}{(E_g+E_{n\ell m})^2-\hbar^2(\omega_1+\omega_2+\mathrm{i}/\tau_{n\ell m})^2}\\
&\times\big(G_{\lambda\mu\nu}(t,t'')F(t'')\big)\big(G_{n\ell m}(t'',t')F(t')\big)\psi^2_{osc,n\ell m}(t).
\end{aligned}
\tag{72}
$$

The formulas (71),(71) are the basic formulas, which describe the properties of 2PA excitons, excited by finite-time laser pulses.

4. Results on Exciton Lifetimes and Other Parameters

4.1 Exciton Lifetimes

We have computed the emission dynamics of Rydberg excitons in Cu_2O created by two-photon absorption. We used the Cu_2O band parameters, collected in Table 1. The first step in the calculations is to establish the

Parameter	Value
E_g	2172.08
R^*	86.96
Δ_{LTS}	5×10^{-2}
m_c	0.99
$m_{h\|\|}$	0.5587
m_{hz}	1.99
$\mu_{\|\|}$	0.3597
μ_z	0.672
a^*	1.1

Table 1: Band parameter values for Cu_2O from [13], energies in meV, masses in free electron mass m0, lengths in nm, ΔLT from [16]. lifetimes of excitons for various exciton states, where we considered the even states S and D. Those lifetimes were measured in [6] and we formulated equations from which the lifetimes can be calculated, for various intervals of the quantum number n. The results are shown in Table A1, and illustrated in Figures 1 and 2. The mentioned above two features of the dependence on the state number, the increase of the lifetime for $n \leq 7$, and a transition to plateau for $n > 7$, are visible.

4.2 Quantum Beatings Periodicity

To explain the oscillations around the envelope describing the excitonic emission delay, the periodicity of these oscillations (quantum beatings) should be calculated. We use the equations (42) and (52). The experimental findings and results of the calculations are presented in Tables A3 and A4.

4.3 The Dependence of Lifetimes on Laser Power and Temperature

The exciton life time is related to the damping constant Γ, being also the linewidth, by the relation

$$\tau = \frac{\hbar}{\Gamma}. \qquad (73)$$

The quantity Γ depends on temperature by relation [10]

$$\Gamma(\mathcal{T}) = \Gamma_0 + \gamma_{AC}\mathcal{T} + \gamma_{LO}\left[\exp(\hbar\omega_{LO}/k_B\mathcal{T}) - 1\right]^{-1}, \qquad (74)$$

where the term $\gamma_{AC}T$ is due to exciton scattering with acoustic phonons, and term nonlinear in temperature is due to interaction with LO phonons. The coefficients γ_{AC} and γ_{LO} represent the strength of the exciton- acoustic phonon interaction, and exciton-LO phonon interaction, respectively, while the term Γ_0 is the low- temperature limit of the line width. As can be seen from (73,74),

$$\frac{d\tau}{d\mathcal{T}} < 0, \qquad (75)$$

which means that the life time decreases with the increasing temperature. By given parameters γ_{AC}, γ_{LO} one can derive an analytical expression for the dependence τ (*T*). The values of coherence times for increasing power can be obtained by the relation

$$\tau_{coh,n} = \tau_0 \exp\left(nb_1 - n^2 b_2 - Wb_3\right). \qquad (76)$$

The coefficients τ_0, b_1, b_2, b_3 (τ_0 in ps, b_3 in 1/mW)

$b_1 = 0.98, \quad b_2 = 0.04,$

$b_3 = 6.6 \times 10{-}3, \quad \tau_0 = 0.394, \quad (77)$

were obtained from fitting experimental results from [6]. The dependence of exciton lifetimes on state number and laser power can be compared with the dependence on temperature and state number. Having in mind the experiments [6], we consider the S states n = 5, 7 and calculate the lifetimes as function of temperature for the given states. We use the formulas.

$$\tau_n(\mathcal{T}) = \mathcal{T}_0 \exp\left(n\gamma_1 - n^2\gamma_2 - \gamma_{3n}\mathcal{T}\right),$$
$$\gamma_{35} = 0.0188, \quad \gamma_{37} = 0.0376, \quad \mathcal{T}_0 \approx 3 \times 10^{-3}$$
$$\gamma_1 = 2.592, \quad \gamma_2 = 0.192, \qquad (78)$$

The results are presented in Table A6.

4.4 Exciton Oscillator Strength

The oscillator strengths for the exciton state |*nlm*> are defined as

$$f_{n\ell m} = \left| \int d^3 r \mathbf{M}(\mathbf{r}) \varphi_{n\ell m}(\mathbf{r}) \right|^2. \qquad (79)$$

For further discussion we must define the shape of the transition dipole density *M*. Since we consider only one component, we take a scalar function. The shape of *M* depends on the considered exciton symmetry. For simplicity, the S exciton function *M* is assumed in the form

$$M(r) = \frac{M_{01}}{4\pi r_0}\delta(r - r_0), \qquad (80)$$

where r_0 is the so-called coherence radius [13], and the coefficient M_{01} is related to the longitudinal transversal splitting energy. An example of the latter is the integrated strength of dipole moment M_{01} for S excitons, obtained from the equation

$$\frac{\Delta_{LTS}}{R^*} = 2\frac{2\mu_{\|}}{\epsilon_0\epsilon_b\pi a^*\hbar^2}M_{01}^2. \qquad (81)$$

The results for S states

$$f_{n00} = \frac{\eta_{00}^3 n(n - \eta_{00}r_0/a^*)^{2(n-1)}}{(n + \eta_{00}r_0/a^*)^{2(n+1)}}, \qquad (82)$$

are displayed in Table A7, for the appropriate η_{00} value. For comparison, we show the oscillator strengths for the isotropic case (η_{00} = 1, r_0 <<a^*) ("pure"), which obey the scaling law $f_{n00} \propto 1/n^3$. The results for η_{00} 6= 1 show a deviation from this law

$$\frac{f_{n00}}{f_{100}} \approx \frac{1}{n^{3.14}}, \quad n = 2, 3, \ldots \qquad (83)$$

For the D excitons we use the transition dipole moment in the form [13]

$$M(r) = M_{02}\frac{Y_{22}}{r^2 r_0}e^{-r/r_0}. \qquad (84)$$

For the considered |*n*22> states the eigenfunction can be put into the form

$$\varphi_{n22}(\mathbf{r}) = N_{n2}Y_{22}(\theta,\phi)\left(\frac{2\eta_{22}}{n}\frac{r}{a^*}\right)^2 \exp\left(-\frac{\eta_{22}r}{na^*}\right), \qquad (85)$$

where N_{n2} are the normalization constants, which enter into the definition of f_{n22} oscillator strengths

$$f_{n22} = M_{02}^2 N_{n2}^2 \left(\frac{2\eta_{22}\rho_0}{n}\right)^4 \exp(-2\eta_{22}\rho_0/n). \quad (86)$$

Their values are listed in Tables A7 and A8. As in the case of S excitons, we show the "pure" values of f_{n22}, obtained for $\eta_{22} = 1$, and given by the relation formula

$$f_{n22} = \left(\frac{2}{n}\right)^7 \left(\frac{1}{5!}\right)^2 \frac{(n+2)!}{2n(n-3)!} \times \text{const},$$
$$\text{const} = M_{02}^2 \rho_0^4 \times 10^{-4}. \quad (87)$$

4.5 Dependence of A and B on the Laser Power

The coefficients A_{nlm}, B_{nlm}, defined in equations (69), depend on the temperature by definitions of λ's

$$\lambda_{th,e} = \left(\frac{\hbar^2}{m_e k_B \mathcal{T}}\right)^{1/2}, \quad \lambda_{th,h} = \left(\frac{\hbar^2}{m_h k_B \mathcal{T}}\right)^{1/2}. \quad (88)$$

They coefficients for hole are determined for the appropriate masses (|| or z), and have the form

$$\bar{\lambda}_{th,e} = \frac{\lambda_{th,e}}{a^*} = \frac{1}{a^*}\left(\frac{2\mu_\parallel \hbar^2}{m_e(2\mu_\parallel)k_B\mathcal{T}}\right)^{1/2} = \left(2\frac{\mu_\parallel R^*}{m_e k_B \mathcal{T}}\right)^{1/2},$$
$$\bar{\lambda}_{th,hz} = \frac{\lambda_{th,hz}}{a^*} = \frac{1}{a^*}\left(\frac{2\mu_\parallel \hbar^2}{m_{hz}(2\mu_\parallel)k_B\mathcal{T}}\right)^{1/2} = \left(2\frac{\mu_\parallel R^*}{m_{hz} k_B \mathcal{T}}\right)^{1/2}, \quad (89)$$
$$\bar{\lambda}_{th,h\parallel} = \frac{\lambda_{th,h\parallel}}{a^*} = \frac{1}{a^*}\left(\frac{2\mu_\parallel \hbar^2}{m_{h\parallel}(2\mu_\parallel)k_B\mathcal{T}}\right)^{1/2} = \left(2\frac{\mu_\parallel R^*}{m_{h\parallel} k_B \mathcal{T}}\right)^{1/2}.$$

The electron effective mass is assumed to be isotropic. As stated in [6], the dependence of coherence and life times on the laser power is equivalent to a dependence on temperature. Therefore we must calculate λ's (89) for various temperatures and, correspondingly, for various laser powers. Since we will use the quantities A;B in calculations of the excitonic emission of exciton 5S state, we will focus the attention on the quantities A_{500};B_{500}. Their calculated values as function of temperature/laser power are displayed in Tables A9 and A10. We observe that these quantities are decreasing with the increasing temperature /laser power.

5. Nonlinear Time Dependent 2P-Absorption Coefficient

Having linear and nonlinear susceptibilities, we obtain the total susceptibility by the relation

$$\chi(\omega_1+\omega_2;t) = \chi^{(1)}(\omega_1,t) + \chi^{(1)}(\omega_2,t) + \chi^{(3)}(\omega_1,t)|\mathcal{E}_{01}|^2 + \chi^{(3)}(\omega_2,t)|\mathcal{E}_{02}|^2. \quad (90)$$

Since the contributions of terms related to ω_1, ω_2, where we take $\omega_1 = \omega_2$, are equal, we denote $\omega_1 + \omega_2 = \omega$. The imaginary part of (90) defines the nonlinear absorption coefficient

$$\alpha_{tot} = \alpha^{(1)}(\omega) + \alpha^{(3)}(\omega)|E_{prop}|^2,$$
$$\alpha^{(1)} = \frac{\hbar\omega}{\hbar c}\mathrm{Im}\,\chi^{(1)}, \qquad (91)$$
$$\alpha^{(3)} = \frac{\hbar\omega}{\hbar c}\mathrm{Im}\,\chi^{(3)}.$$

where $|E_{prop}|^2 = |s_0 1|^2 = |s_0 2|^2$. Having in mind the experiments[7], we will consider the absorption for a given exciton state *nlm*. Using (81) and (58), we obtain for S-states

$$\alpha^{(1)}_{n00}(t) = \alpha^{(1)'}_{n00}\big(G_n(t,t')F(t')\big)\psi_{osc,n00}(t), \qquad (92)$$

where

$$\alpha^{(1)'}_{n00} = \frac{\hbar\omega}{\hbar c}\sqrt{\epsilon_b}\Delta_{LTS}\frac{f_{n00}\Gamma_{n00}}{2E^2_{n00}}. \qquad (93)$$

For the nonlinear contribution we obtain

$$\chi^{(3)}_n(\omega,t) = -\frac{2M_0^2}{\epsilon_0}\frac{c_n(A_n+B_n)(E_n+E_g)}{E_n^2}$$
$$\times\frac{T_1}{\tau_n}\frac{c_n\varphi_n(0)(E_n+i\Gamma_n)}{2E_g(E_n^2+\Gamma_n^2)}$$
$$\times(G_n(t,t'')F(t''))(G_n(t'',t')F(t'))\psi^2_{osc,n}(t) \qquad (94)$$

Similar expression holds for the D-exciton contribution. Absorption coefficient $\alpha^{(3)}_{n00}$ obtained from the imaginary part of (94), has the form

$$\alpha^{(3)}_n = -\alpha^{(1)'}_n\chi^{(3)'}_n|E_{prop}|^2$$
$$\times\big(G_n(t,t'')F(t'')\big)\big(G_n(t'',t')F(t')\big)\psi^2_{0sc,n}(t), \qquad (95)$$
$$\chi^{(3)'}_n = \epsilon_0\epsilon_b\Delta_{LTS}a^{*3}\frac{1}{E_-^2+4\Gamma_-^2}\frac{T_1}{\tau_n}\varphi_n(\rho_0)(A_n+B_n).$$

We use the relation

$$|E_{prop}|^2 = 6\times10^8 W, \quad [W] = \mathrm{mW}, \qquad (96)$$

appropriate for $20\,\mu$m laser spot diameter, and separating the parameters appropriate for Cu_2O, obtaining for nS states

$$\alpha^{(3)}_n = -\alpha^{(1)'}_n\left\{\left(\frac{t_1}{\tau_n}\right)[\varphi_n(\rho_0)(A_n+B_n)]\right.$$
$$\times\ 2.745\times10^{-8}\left(\frac{n}{\eta_{00}}\right)^4\times W \qquad (97)$$
$$\left.\times\ (G_n(t,t'')F(t''))(G_n(t'',t')F(t'))\psi^2_{osc,n}(t)\right\}$$

where

$$t_1 = 10^{-3}T_1.$$

In calculations we use a Gaussian shaped normalized pulse

$$F(t) = F_{max}\frac{1}{\tau_p\sqrt{2\pi}}\exp\left(-\frac{t^2}{2\tau_p^2}\right), \qquad (98)$$

where τ_p is the pulse temporal duration. Using this shape we calculate the expressions $G_n(t,t')$ $F(t')$ and, in a lowest approximation, we obtain the time dependence of the normalized emission in the form

$$I_n(t,W) = N_n \exp\left(-\frac{|t|}{\tau_n}\right)\frac{\psi_{n,osc}(t)}{Q_n} \qquad (99)$$
$$\times\left\{1-\chi_n^{(3)'}We^{b_3W}[\varphi_n(\rho_0)(A_n+B_n)]\psi_{osc,n}(t)\right\},$$

where N_n are normalization constants

$$\chi_n^{(3)'} = \left(\frac{t_1}{\tau_n'}\right)\left(\frac{n}{\eta_{00}}\right)^4 2.475\times10^{-8}. \qquad (100)$$

The theoretical results are illustrated in Figure 4 for 5S state and three values of the applied laser power. We observe an exponential decay, governed by the exponent $-1/\tau_5$, and quantum beats. The details of calculation are given in Appendix.

6. Fourier transform

Having an analytical form for the oscillating functions $\psi_{n,osc}(t)$ one can easily calculate the Fourier transform of these functions. Using the standard definition

$$F(\xi) = \frac{1}{\sqrt{2\pi}}\int_{-\infty}^{\infty} f(x)e^{i\xi x}dx,$$

and substitute $t \to x, \quad \xi \to \omega$ we obtain

$$f(x) = \sum_j q_{jn}e^{-a_n|x|}\cos(\Omega_{jn}x),$$
$$a_n = \frac{1}{\tau_n},$$

where j runs over the considered transitions. Then

$$F_n(\omega) \propto \sum_j \frac{q_{jn}}{a_n^2+(\Omega_{jn}+\omega)^2}. \qquad (101)$$

The above expression will be applied for the cases of 4D and 6S excitons. In the case of 4D excitons we use the frequencies corresponding to the transitions $n_1S \to n_2D$, where $n_1 = 3; 4; 5$, and $n_2 = 4; 1; 4; 2; 5; 1; 5; 2$, which are displayed in Tables A3 and A4. With the above data we obtain the expression for the Fourier transform for 4D

$$F_{D4} = 28.2\left[1+\frac{0.0476}{1+7000(\nu-0.06)^2}\right.$$
$$+\frac{0.32}{1+7000(\nu-0.207)^2}+\frac{0.397}{1+7000(\nu-0.28)^2}$$
$$\left.+\frac{0.105}{1+7000(\nu-0.365)^2}+\frac{0.132}{1+7000(\nu-0.295)^2}\right].$$

For the 6S excitons we obtain

$$F_{S6} = 14\left[\frac{0.5}{1+3947(\nu-0.09)^2}+\frac{0.345}{1+3947(\nu-0.09)^2}\right.$$
$$+\frac{0.079}{1+3947(\nu-0.134)^2}+\frac{0.06}{1+3947(\nu-0.178)^2}$$
$$\left.+\frac{0.007}{1+3947(\nu-0.188)^2}\right]. \qquad (102)$$

The corresponding Fourier transforms are presented in Figures 6 and 7. In both cases the factors were chosen to be proportional to the transition quadrupole moments for $n_1S \to n_2D$ [8]. The numbers 28.2 in (102) and 14 in (102) give the fit to the transform obtained

numerically from experimental curve. We considered the quadrupole moments for the transitions $n_1S \rightarrow n_2D_2$ states, due to the symmetry properties of D_2. The state D_1 is not a pure D state, but reveals a mixing with nearest P state [17]. Therefore the quadrupole moment for the transition $n_1S \rightarrow n_2D_1$ has a smaller value than the moment $n_1S \rightarrow n_2D2$. We assumed the rate 0.8, which of D2. The state D_1 is not a pure D state, but reveals a mixing with nearest P state [17]. Therefore the quadrupole moment for the transition $n_1S \rightarrow n_2D_1$ has a smaller value than the moment $n_1S \rightarrow n_2D_2$. We assumed the rate 0.8, which corresponds to the experimental observations. For the D4, 1→ D4, 2 we used the quadrupole moment for the P4 →S4 transition, due to the above described mixing of states. We observe the property mentioned in [6], that the oscillations are typically dominated by a main frequency accompanied by few others of smaller amplitude. It is due to the structure of amplitudes qjn (54), where the major contribution comes from the state transitions nS → *nD2* for n ≤ 5 and nS → nD1 for n ≥ 6, see also Tables I, II [8].

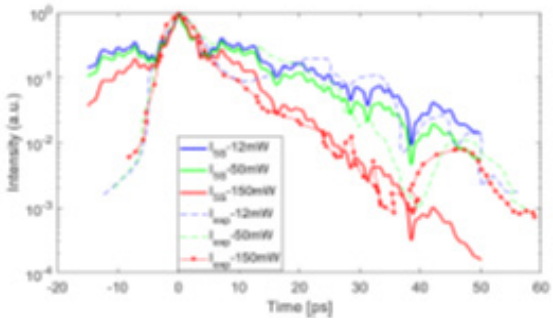

Figure 5: Linear time dependent emission for the state 5S and three applied laser powers

7. Conclusions

This study contains derivation of analytical expressions describing the direct measurements of lifetimes of the even series of Rydberg excitons in Cu_2O. We obtained formulas which show the power scaling laws for excitons S, D1, and D2 for the lower exciton states ($n < 6$) and a saturation effect for $n > 6$ states, explaining origins of this effect. Using the real density matrix approach, we derived formulas for the time dependence of linear and nonlinear susceptibility, under action of pulsed excitation. Both susceptibilities show the effect of quantum beats. The time evolution shows an exponential decay, governed by the exciton life time. In addition, we described the lifetimes dependence on the applied laser power and the crystal temperature. Having analytical expression for the nonlinear susceptibility $\chi(3)$, we can calculate the nonlinear refraction index n2(W), which enables the study of Kerr-type nonlinearities [11].

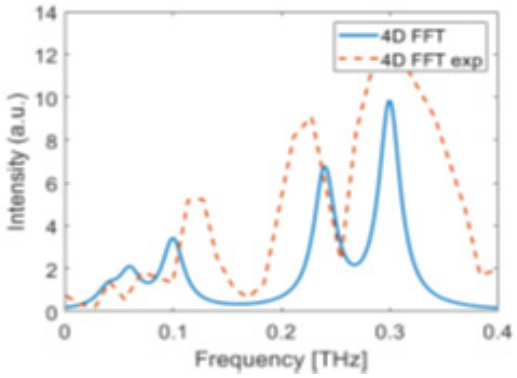

Figure 6: Fourier transform of the I4D emission function

Figure 7: Fourier transform of the I6S emission function

Appendix A: Calculation Details

Appendix A.1: Exciton Lifetimes

We have calculated the exciton lifetimes using the equations (26), (29),(40,41,42) and the values of $\mu_{\|}$, μz from the Table 1, obtaining for the coefficient η00, relevant for S excitons

$$\eta_{00} = 0.5 \int_0^{\pi} \frac{\sin\theta d\theta}{\sqrt{\sin^2\theta + (\mu_{\|}/\mu_z)_2 \cos^2\theta}} = 1.1. \quad (A.1)$$

The case od D excitons is more complicated. If the exciton S can be considered as non-degenerate, for D excitons the band structure must be taken into account. The D states reveal a splitting, where one state has a larger energy than other with the same principal quantum number. We choose two states, which result from group-theoretical considerations [17], with representations(here for the state 4D) 4DΓ+Γ+(3/2) (state 4D1), and 4DΓ+(5/2) (state D2). The symmetry properties are reflected by in the Luttinger equations for the hole effective masses (in Cu2O the electron mass is assumed to be isotropic)

$$m_{hz} = \frac{m_0}{\gamma_1 - 2\gamma_2},$$
$$m_{h\|} = \frac{m_0}{\gamma_1 - 2\gamma_3}. \quad (A.2)$$

We take $\gamma_2 \neq \gamma_3$for the D1 state, and $\gamma_2 = \gamma_3$for the D2 state. Using the values $\gamma_1 = 1.79, \gamma_2 = 0.82, \gamma_3$ = 0:54 [18], we obtain $\mu_{\|}/\mu_z$ = 0:673 for the D1 state and $\mu_{\|}/\mu_z$= 1 for the D2 state, and

$$\eta_{22,1} = \frac{15}{16} \int_0^{\pi} \frac{\sin^5\theta d\theta}{\sqrt{\sin^2\theta + 0.673\cos^2\theta}} = 1.02555,,$$
$$\eta_{22,2} = \frac{15}{16} \int_0^{\pi} \frac{\sin^5\theta d\theta}{\sqrt{\sin^2\theta + \cos^2\theta}} = 1. \quad (A.3)$$

Table A3: Exciton beatings characteristic frequencies of the II type

$\nu = (\tau_{qb,n_1,n_2})^{-1}$ corresponding to $(n_2\mathrm{D} \rightarrow n_1\mathrm{S})$ transitions

$n_2D\downarrow/n_1S\rightarrow$	3	4	5	6	7
3,1	0.368	0.8			
3,2	0.448	0.9			
4,1		0.207	0.365		
4,2		0.278	0.295		
5,1			0.132	0.178	
5,2			0.17	0.134	
6			0.4	0.09	0.09
7				0.254	0.067

The results are reported in Tables A1 and A2, and illustrated in Figures 1 and 2. For $n > 5$ we have chosen the values for D1. In Table A3 we present the values of quantum beats frequencies of the II type, calculated with the formula (20). For the lowest exciton states 3 n 5 the splitting D→D_1,D_2 is accounted for, thus Δ_{n1} = E(nD1) E_{n00}, Δ_{n2} = E(nD2) E_{n00} and, correspondingly, $\tau_{qb,n1}$, $\tau_{qb,n2}$, for n > 5 Δ_{n1} = respectively. In addition, we have calculated some examples of frequencies of the I type beats (values in ps):

$$\nu_{S67} = 0.188 \quad \mathrm{S6} \rightarrow \mathrm{S7},$$
$$\nu_{D41} = 0.06 \quad \mathrm{D4,1} \rightarrow \mathrm{D4,2}. \quad (A.4)$$

Appendix A.2: The Dependence on Temperature and the Laser Power

Since the crystal temperature is assumed to be proportional to the applied laser power W , we treat the exciton lifetimes shown in Table A1 as the values at T= 0, and calculate the coherence times as functions of the applied laser power by equation (76 The results are given in Table A5. The dependence of exciton lifetimes on state number and laser power can be compared with the dependence on temperature and state number. Having in mind the experiments reported in [6], we consider the S states n = 5, 7 and calculate the lifetimes as function of temperature for the given states. We use the formulas

$$\tau_n(\mathcal{T}) = \mathcal{T}_0 \exp\left(n\gamma_1 - n^2\gamma_2 - \gamma_{3n}\mathcal{T}\right),$$
$$\gamma_{35} = 0.0188, \quad \gamma_{37} = 0.0376, \quad \mathcal{T}_0 \approx 3 \times 10^{-3}, \quad \text{(A.5)}$$
$$\gamma_1 = 2.592, \qquad \gamma_2 = 0.192.$$

The results are presented in Table A6.

S	E_{Tn00}	E_{n00}	Exp.τ_{n00}	(41)	(42)	(43)
2	2145.77	26.3	0.7 ± 0.12	0.88	0.84	0.96
3	2160.4	11.69	3.1 ± 1	2.54	2.52	3.08
4	2165.5	6.58	5.1 ± 0.2	5.48	5.51	6.64
5	2167.87	4.2	11.4 ± 2	10.08	10.11	11.17
6	2169.157	2.92	19 ± 1.5	16.72	16.61	15.69
7	2169.93	2.147	20 ± 1.5	25.76	25.26	19.24
8	2170.436	1.644	21.5 ± 2	37.57	36.32	21.42
9	2170.78	1.3	22 ± 2.5	52.53	50.04	22.43

Table A1: Exciton S (|n00⟩) eigenenergies En00, resonances ET n00 (meV), and lifetimes τn00 (ps), comparison of experimental data (Exp.) [6] and results of different scalings, obtained from equations (41-43)

D	E_{Tn22}	E_{n22}	Exp.τ_{n22}	(41)	(42)	(43)
3,1	2161.92	10.29	3.2 ± 0.2	2.92	3.01	3.2
3,2	2162.42	10.41	3.2 ± 0.2	2.91	2.97	3.7
4,1	2166.36	5.86	5.7 ± 0.5	6.3	6.6	6.89
4,2	2166.65	5.79	5.7 ± 0.5	6.3	7.04	7.97
5,1	2168.42	3.75	10.5 ± 0.9	11.59	12.14	11.56
5,2	2168.6	3.70	10.5 ± 0.9	13.1	13.75	13
6	2169.54	2.57	17.5 ± 1.2	18.39	19.976	17.58
7	2170.21	1.89	19 ± 1.5	28.8	30.4	19.92
8	2170.65	1.45	22 ± 2	41.07	43	22.31
9	2170.95	1.14	23 ± 2.5	47.39	60.4	23.27

Table A2: Exciton D (|n22⟩) eigenenergies E_{n22}, resonances E_{Tn22} (meV), and lifetimes τn22 (ps) for both types of exciton D, comparison of experimental data (Exp.) [6] and results of different scalings, obtained from equations (41)-(43). The experimental values for D1, D2 excitons $(|n22\rangle_{1,2})$ from [6]

$n' \downarrow / n_1 S \rightarrow$	3	4	5	6	7
3,1	2.31	5			
3,2	2.815				
4,1		1.3	2.29		
4,2		1.747	1.853		
5,1			0.829	1.118	
5,2			1.068	0.842	
6			2.51	0.56	0.56
7				1.6	0.42

Table A4: Exciton beatings characteristic frequencies Ω_{n1n2} of the II type corresponding to ($n_2D \rightarrow n_1S$) transitions

n/W	0	12	50	150
3	2.6	2.4	1.86	0.96
4	5.23	4.83	3.76	1.94
5	9.73	9.0	7.0	3.61
6	16.7	15.43	12	6.2
7	26.45	24.44	19.0	9.8

Table A5: Lifetimes τn_{00} vs laser power W (τn_{00} in ps, W in mW)

$\mathcal{T}/\tau_n$	Exp. τ_5	Th.	Exp. τ_7	Th.
0		10.49		18.66
5	9 ± 2	9.55	14 ± 2	15.47
8	8 ± 2	9.0	13 ± 2	13.8
10	7.5 ± 2	8.7	15 ± 2	12.8
15	7.5 ± 2	7.9	13 ± 2	10.6
20	7 ± 2	7.2	13 ± 2	8.8
30	6 ± 2	5.97	9 ± 2	6.04
40	5 ± 2	4.94	4 ± 2	4.14
50	3 ± 2	4.09	73 ± 2	2.84

Table A6: Lifetime vs temperature, n = 5, 7(|500⟩, |700⟩), experimental data from [6], theoretical results from Eq. (78), times in ps, temperature in K

States	f_{n00}/f_{100} "pure"	Th.
$\|100\rangle$	1	1
$\|200\rangle$	1/8	1/8.4
$\|300\rangle$	1/27	1/30
$\|400\rangle$	1/64	1/67
$\|500\rangle$	1/125	1/131
$\|600\rangle$	1/216	1/227
$\|700\rangle$	1/343	1/360
$\|800\rangle$	1/512	1/538

Table A7: Oscillator strengths fn00 “pure”, and results of calculations (82) (Th, in terms of M^2_{01}) and A8 we present the results of calculations of exciton oscillator strength for S and D exciton.

Appendix A.3: Linear and Nonlinear Polarization, Time Dependence

The time evolution of exciton population at the given exciton state is described by the equation (99). Below we present the formulas derived from the mentioned

States	f_{n22} pure	Results
$\|322\rangle$	0.81	0.83
$\|422\rangle$	0.48	0.57
$\|522\rangle$	0.28	0.34
$\|622\rangle$	0.18	0.21
$\|722\rangle$	0.12	0.18
$\|822\rangle$	0.08	0.122

Table A8: Oscillator strengths f_{n22} “pure” ((88) manuscript), and results of calculations (Results, (87) manuscript), all oscillator strength multiplied by 10^{-4} $M^2_{02}\rho^4_0$))

W	$\mathcal{T}$	$\lambda_{th,e}$	$\lambda_{th,hz}$	$\lambda_{th,h\parallel}$
12	10	73	36.48	129
50	20	36	18.24	64.97
100	40	18.33	9.12	32.48
150	50	14.66	7.29	26.0

Table A9: Variation of λ's defined in equations (87) in the manuscript, with the laser power and temperature

Laser power	$A_{500\varphi 500}$	$B_{500\varphi 500}$	$(A+B)_0$
12	27.76	27.45	55.21
50	16.9	17.6	34.5
100	3.516	5.16	8.67
150	1.14	2.59	3.73

Table A10: Quantities $A_{500\phi 500}(\rho 0)$, $B_{500\phi 500}(\rho 0)$, $(A+B)0 = (A5_{00\phi 500} + B5_{00\phi 500})$, laser power in mW, equation for the data of 4D (I_{4D}) and 6S (I_{6S} excitons (linear part only)

$$I_{4D} = 0.625 \exp\left(-0.11\sqrt{(t-1)^2+0.3}\right)$$
$$\Big[1 + 0.0476\cos(0.377\,t)$$
$$+ 0.32\cos(1.3\,t) + 0.3987\cos(1.76\,t) \qquad (A.6)$$
$$+ 0.105\cos(2.29\,t) + 0.132\cos(1.85\,t)\Big],$$

$$I_{6S} = \exp\left(-0.1\sqrt{(t-1)^2+0.3}\right)\Big[1 + 0.684\cos(0.25\,t)$$
$$+ 0.0074\cos(0.377\,t) + 0.148\cos(0.628\,t) \qquad (A.7)$$
$$+ 0.296\cos(1.5\,t) + 0.44\cos(1.88\,t)\Big].$$

Note that the lifetimes τ_n are taken for laser power 50mW. The resulting line shapes are displayed in Figures 3 and 4. When the nonlinear part is accounted for, we first must determine the dependence of quantities A_n, B_n on the laser power (probe temperature). We perform the calculations for the 5S state. Using the quantities λ (Table A9) we obtain the A_{500}, B_{500} values (Table A10). For the S5 state we obtain $\tau' = 9.73$, and

$$\varphi_5(\rho_0)(A_5 + B_5) = 71\,\exp(-0.021\,W). \qquad (A.8)$$

Separating the parameters appropriate for the state 5S, and taking t1 = 0.5, we obtain

$$\chi^{(3)}_{05} = 2.745\times 10^{-8}\left(\frac{0.5}{9.73}\right)e^{b_3 W}$$
$$\times\,[\varphi_5(\rho_0)(A_5+B_5)]\left(\frac{5}{1.1}\right)^4$$
$$= W\exp(-0.0144W)\times 3.85\times 10^{-5}.$$

Using the function ψ_{osc},5(t) in the form ((52), manuscript)

$$\psi_{osc,5} = 713 \times \tilde{\psi}_{osc,5}(t),$$
$$\tilde{\psi}_{osc,5}(t) = 1 + 0.285\cos(0.829\,t)$$
$$+ 0.356\cos(1.068\,t) + 0.277\cos(2.51t) \qquad \text{(A.9)}$$
$$+ 0.036\cos(2.29\,t) + 0.045\cos(1.85\,t),$$
$$\tau_{500}(12) = 9, \quad \tau_{500}(50) = 7, \quad \tau_{500}(150) = 3.61,$$

We obtain the total normalized emission (99), for the 5S exciton, in the form

$$I_5(t,W) = N_{05}\exp\left(-\frac{|t|}{\tau_5}(W)\right)\tilde{\psi}_{osc,5}(t) \qquad \text{(A.10)}$$
$$\times\left[1 - X(W)\tilde{\psi}_{osc,5}(t)\right],$$
where
$$X(W) = 2.745\times 10^{-2} W\exp(-0.0144W)$$
$$\approx 0.87\exp\left[0.035\,W - \left(1.925\times 10^{-4}\right)W^2\right], \qquad \text{(A.11)}$$

and N_{05} is a normalization constant. As can be seen from the above equation, the function X(W) has a Gaussian shape, with X(12) = 0.277 and the maximum at W≈90. Than the function decreases to X(150) = 0.468.

References

1. Kazimierczuk T Fröhlich D Scheel S Stolz H and Bayer M 2014 Giant Rydberg excitons in the copper oxide Ct120 Nature 514 343-347
2. Thewes J Heckötter J Kazimierczuk T Aßmann M Fröhlich D Bayer M. Semina M A and Glazov M M 2015 Observation of High Angular Momentum Excitons in Cuprous Oxide Phys. Rev. Lett. 115, 027402 (2015)
3. Aßmann M and Bayer M 2020 Semiconductor Rydberg Physics, Advanced Quantum Technologies 1900134
4. Konzelmann A Frank B and Giessen H 2020 Quantum confined Rydberg excitons in reduced dimensions J. Phys. B: At. Mol. opt. Phys. 53 024001
5. Ziemkiewicz D Karpifiski K Czajkowski G and ZielifiskaRaczyfiska S 2020 Excitons in Cu20; From quantum dots to bulk crystals and additional boundary conditions for Rydberg exciton-polaritons Phys. Rev. B 101 205202
6. Ziemkiewicz D Czajkowski G and Zielifiska-Raczyfiska S 2024 Optical properties of Rydberg excitons in Cu20based superlattices Phys. Rev. B 109, 085309
7. Chakrabarti P Morin K Lagarde D Marie X and Boulier T 2025 Direct measurement Of the lifetime and coherence time of Cu20 Rydberg excitons Phys. Rev. Lett. 134, 126902
8. Zielifiska-Raczyfiska S and Ziemkiewicz D 2025 Quantum interference of Rydberg excitons in Cu20: Quantum beats Phys. Rev. B 111 205201
9. Tait W C 1972 Quantum theory of a basic light-matter interation Phys. Rev. B 648
10. Zhao H Wachter S and Kalt H 2002 Effect of quantum confinement on exciton-phonon interactions Phys. Rev. B 42 11218
11. Heckötter J Panda B Brågelmann K Aßmann M and Bayer M 2024 Temperature Study of High-n Rydberg States in Cu20 Adv. Quantum Technol. 2300426 DOI:10.1002/qute.202300426
12. Stolz H Schöne F and Semkat D 2018 Interaction of Rydberg excitons in cuprous oxide with phonons and photons: optical linewidth and polariton effect New J. Phys. 20 023019
13. Heckötter J Rommel P Main J Aßmann M and Bayer M 2021 Impact of band mixing on the fine structure of the D-exciton shell in cuprous oxide Physica Status Solidi (RRL) - Rapid Research Letters 15 2100335
14. Ziemkiewicz D Knez D Garcia E P Zielifiska-Raczyfiska S Czajkowski G Salandrino A Kharintsev S S Noskov A 1 Potma E O and Fishman D A 2024. Photon Absorption in Silicon Using Real Density Matrix Approach Journ. Chem. Phys. 161 144117
15. Zielifiska-Raczyfiska S Czajkowski G and Ziemkiewicz D 2016 Optical properties of Rydberg excitons and polaritons Phys. Rev. B 93 075206
16. Morin C Tignon J Mangeney J Dhillon S Czajkowski G

Karpifiski K Zielifiska-Raczyfiska S Ziemkiewicz D and Boulier T 2022 Self-Kerr effect across the yellow Rydberg series of excitons in Cu20 Phys. Rev. Lett. 129 137401

17. Bassani F and Parravicini G P 1975 Electronic States and Optical Trunsitions in Solids (Pergamon Press Oxford) Schweiner F Main J Wunner G and Uihlein C 2017 Even exciton series in Cu20 Phys. Rev. B 95 195201
18. Klingshirn C 2012 Semiconductor Optics (Berlin, Springer)